Chaotic signals representation and spectral characterization using linear discrete-time filters

1st Rafael Alves da Costa
Telecommunication and Control Engineering Department
Escola Politécnica, University of São Paulo
São Paulo, Brazil
ORCID: 0000-0002-1204-9595

2nd Marcio Eisencraft
Telecommunication and Control Engineering Department
Escola Politécnica, University of São Paulo
São Paulo, Brazil
ORCID: 0000-0001-8415-707X

***Abstract*—We present a discrete-time linear recursive filter representation for a piecewise-linear map that generates chaotic signals. It can be used to easily deduce analytical formulas for power spectral density of chaotic signals, providing useful results for chaos-based communication systems and signal processing. Numerical simulations are used to validate the theoretical results.**

***Index Terms*—chaotic signals, nonlinear systems, power spectral density, recursive filters.**

I. Introduction

Discrete-time nonlinear dynamic systems that generate chaotic signals [1] have been considered in many signal processing applications, such as wireless and underwater communications [2]–[8], radar [9], image encryption [10], watermarking [11], among others. The main motivation for these applications is the fact that chaotic signals can increase security by exploring the properties of nonlinear dynamics [6], [12].

To turn these applications viable, it is fundamental to precisely obtain the power spectral density (PSD) of chaotic signals and their bandwidth. These are not easy tasks due to their nonlinear nature and the lack of closed-form expressions for their time evolution. Although some results were recently obtained [13]–[15], more general results are still under investigation.

The general idea of [13]–[15] is to obtain recursive formulas for the n-th iterate of piecewise-maps leading to expressions for the autocorrelation sequence and, consequently, for the PSD. We consider here a different approach, based on the work of Drake and Willians [16]. They have shown that it is possible to obtain chaotic signals using discrete-time recursive linear filters. More precisely, they use a filter to successfully generate chaotic orbits of the sawtooth map in the $[0, 1[$ interval.

In the present paper, we extend this linear representation to a class of piecewise-linear maps with positive or negative slopes. Next, we use it to derive the PSD of chaotic signals directly. It is organized as follows: In Section II, the considered piecewise linear map is presented. In Section III its linear representation is deduced and exemplified. In Section IV it is used for PSD calculation. Finally, in Section V, we draft some conclusions and point to future works.

This study was financed in part by the Coordenação de Aperfeiçoamento de Pessoal de Nível Superior - Brasil (CAPES) - Finance Code 001. M.E. was partially financed by CNPq-Brazil, Grant 311039/2019-7.

II. Considered Map

Let $f : [-1, 1[\to [-1, 1[$ be defined as

$$f(s) = 2g\left(r\frac{s+1}{2}\right) - 1, \tag{1}$$

with

$$g(y) = y - \lfloor y \rfloor \tag{2}$$

and r integer with $|r| \geq 2$.

We consider the map

$$s(n+1) = f(s(n)), \tag{3}$$

for $n \geq 0$ and $s(0) \in [-1, 1[$. It is a generalization of the the sawtooth map used in [16], allowing for negative r and a symmetric domain with zero-mean generated signals.

Figure 1(a) shows $f(s)$ for $r = -3$. Figure 1(b) presents the generated signals for $s(0) = -0.73$ and $s(0) = -0.73000001$. It can be clearly observed that the orbits are bounded, aperiodic and present sensitive dependence on initial conditions, characteristics of chaotic signals [1].

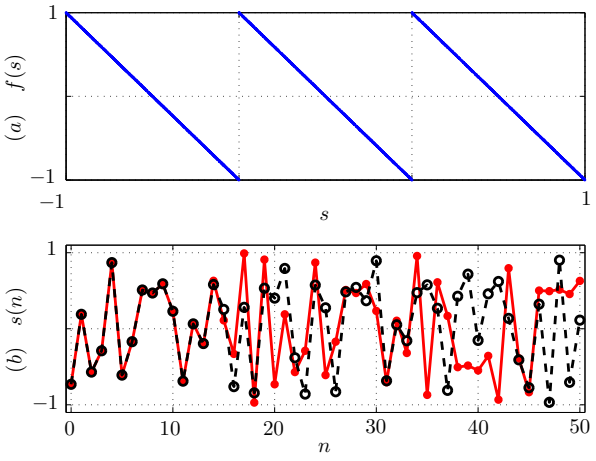

Fig. 1. (a) Graphic of $f(s)$ (1) for $r = -3$. (b) Two generated signals with close initial conditions.

The map f can be decomposed in three:

- $x(n) = \frac{s(n)+1}{2} = f_1(s(n))$ - linear transformation of the domain from $[-1, 1[$ to $[0, 1[$;
- $x(n+1) = f_2(x(n)) = g(rx(n))$;
- $s(n+1) = 2x(n+1) - 1 = f_3(x(n+1)) = f_1^{-1}(x(n+1))$- linear transformation from $[0, 1[$ to $[-1, 1[$;

so that $f = f_3 \circ f_2 \circ f_1$.

As $f_1(\cdot)$ and $f_3(\cdot)$ are inverse functions,

$$s(n) = f^n(s_0) = (f_3 \circ f_2 \circ f_1)^n(s_0) = (f_3 \circ g^n \circ f_1)(s_0). \tag{4}$$

For positive r, $f_2(\cdot) = g(\cdot)$ consists in a shifting in the base-r representation of $x(n)$, i.e., if

$$x(0) = \sum_{k=0}^{\infty} \frac{d_k}{r^{k+1}} = (0, d_0 d_1 d_2 \ldots)_{|r|}, \tag{5}$$

then $x(1) = (0, d_1 d_2 d_3 \ldots)_{|r|}$, with $0 \leq d_k < |r|$, so that

$$x(n) = \sum_{k=0}^{\infty} \frac{d_{k+n}}{r^{k+1}}, \tag{6}$$

For negative r, there is also a complementary operation, i.e., $x(n+1) = 1 - (0, d_1 d_2 d_3 \ldots)_{|r|}$. Thus, for n even the samples $x(n)$ for the map with parameter $|r|$ or $-|r|$ are the same. For n odd they are complements in base $|r|$. This way, defining

$$d'_k = \begin{cases} -(d_k + 1), & k \text{ even} \\ d_k - |r|, & k \text{ odd} \end{cases}, \tag{7}$$

it can be shown that

$$x(n) = \sum_{k=0}^{\infty} \frac{d'_{k+n}}{r^{k+1}}. \tag{8}$$

In the next sections, we develop a linear representation for this map and use it to obtain the PSD of $s(n)$.

III. Linear representation

Algorithm 1 systematizes the proposal of generating an estimate $\hat{s}(n)$, $n = 0, 1, 2, \ldots, N-1$ of (3) of $s(n)$ given r, N and $s(0)$ using a linear filter.

As a first step, the initial condition $s(0) \in [-1, 1[$ is linearly transformed in $x(0) \in [0, 1[$ using $f_1(\cdot)$ (9). Then $x(0)$ is decomposed on base $|r|$ with digits d_k. Using d_k, the algorithm specifies an entrance $v(n)$ for the linear filter described in (13) whose output is $x_\ell(n)$.

Solving (13) with $x_\ell(-1) = 0$, we obtain [17]

$$x_\ell(n) = \sum_{j=0}^{n} \frac{v(j)}{r^{n-j+1}}. \tag{15}$$

Finally, an estimate $\hat{s}(n)$ for the orbit with initial condition $s(0)$ is obtained in (14) by flipping $x_\ell(n)$ and applying $f_1^{-1}(\cdot)$ in (14).

Theorem 1 gives a higher bound for $|s(n) - \hat{s}(n)|$.

Algorithm 1: Obtaining the signal $\hat{s}(n)$ using linear filter.

Data: r, N, $s(0)$, $x_\ell(-1) = 0$.
Result: $\hat{s}(n)$, for $n = 0, 1, 2, \ldots, N-1$.
begin

$$x(0) \leftarrow \frac{s(0)+1}{2} \tag{9}$$

Decompose $x(0)$ in base $|r|$, writing it as

$$x(0) = (0, d_0 d_1 d_2 \ldots d_{N-1} \ldots)_{|r|}, \tag{10}$$

with $d_k \in \{0, 1, \ldots, |r|-1\}$, $k = 0, 1, \ldots, N-1$.

for $n = 0, 1, 2, \ldots, N-1$ **do**

  if $r > 0$ **then**

$$v(n) \leftarrow d_{N-1-n} \tag{11}$$

  else

$$v(n) \leftarrow d'_{N-1-n} = \begin{cases} -(d_{N-1-n}+1), & n \text{ even} \\ d_{N-1-n} - |r|, & n \text{ odd} \end{cases} \tag{12}$$

$$x_\ell(n) \leftarrow \frac{1}{r}\left[x_\ell(n-1) + v(n)\right] \tag{13}$$

for $n = 0, 1, 2, \ldots, N-1$ **do**

$$\hat{s}(n) \leftarrow 2x_\ell(N-1-n) - 1 \tag{14}$$

Theorem 1 (Main result): Let $s(n)$, $0 \leq n \leq N-1$ obtained using (3) with initial condition $s(0)$ and fixed r and $\hat{s}(n)$ generated by Algorithm 1 with same parameters. Then,

$$\varepsilon(n) = |s(n) - \hat{s}(n)| \leq |r|^{n-N}, \tag{16}$$

for $0 \leq n \leq N-1$.

Proof: We divide the proof in two cases:

A) $r \geq 2$

Applying $f_1(\cdot)$ in (14) and using (15) and (11),

$$\hat{x}(n) = x_\ell(N-1-n) = \sum_{j=0}^{N-1-n} \frac{d_{N-1-j}}{r^{N-1-n-j+1}}. \tag{17}$$

Defining $k = N-1-n-j$, we get

$$\hat{x}(n) = \sum_{k=0}^{N-1-n} \frac{d_{k+n}}{r^{k+1}}. \tag{18}$$

From (6) and (18) and bearing in mind that $d_k \leq r-1$, we obtain

$$\varepsilon(n) = \left| \sum_{k=0}^{\infty} \frac{d_{k+n}}{r^{k+1}} - \sum_{k=0}^{N-1-n} \frac{d_{k+n}}{r^{k+1}} \right| = \left| \sum_{k=N-n}^{\infty} \frac{d_{k+n}}{r^{k+1}} \right|$$
$$\leq \left| (r-1) \sum_{k=N-n}^{\infty} r^{-(k+1)} \right|$$
$$\leq \left| (r-1) \frac{r^{-(N-n+1)}}{\left(1-\frac{1}{r}\right)} \right| = |r|^{n-N}. \quad (19)$$

B) $r \leq -2$

Applying $f_1(\cdot)$ in (14) and using (15) and (12)

$$\hat{x}(n) = x_\ell(N-1-n) = \sum_{j=0}^{N-1-n} \frac{d'_{N-1-j}}{r^{N-1-n-j+1}}. \quad (20)$$

Defining $N-1-n-j=k$, we get

$$\hat{x}(n) = \sum_{k=0}^{N-1-n} \frac{d'_{k+n}}{r^{k+1}}. \quad (21)$$

Using (21) and (8) we have

$$\varepsilon(n) = \left| \sum_{k=0}^{\infty} \frac{d'_{k+n}}{r^{k+1}} - \sum_{k=0}^{N-1-n} \frac{d'_{k+n}}{r^{k+1}} \right| = \left| \sum_{k=N-n}^{\infty} \frac{d'_{k+n}}{r^{k+1}} \right|. \quad (22)$$

For n even and odd, we have $1 \leq \left|d'_{k+n}\right| \leq |r|$ in (22). It follow that

$$\varepsilon(n) \leq \sum_{k=N-n}^{\infty} \frac{\left|d'_{k+n}\right|}{|r|^{k+1}} = \frac{|r|^{n-N}}{1-|r|} \leq |r|^{n-N}. \quad (23)$$

■

As an example, consider $r=-3$, $N=51$ and

$$s(0) = \frac{2}{\pi} - 1. \quad (24)$$

Thus,

$$x(0) = (s(0)+1)/2 = 1/\pi = (0, 0221210010\ldots)_3. \quad (25)$$

Figure 2(a) shows d_n, Figure 2(b) shows the input to the linear filter $v(n)$, Figure 2(c) the orbits generated using the nonlinear map and the linear filter and, finally, the error $\varepsilon(n)$ along with its upper bound (16) are presented in Figure 2(d). Note that for $n<20$, $\varepsilon(n)$ is under the our machine precision (10^{-16}) and is not shown.

IV. Power Spectral Density

Analytical results for the PSD of chaotic signals generated by piecewise-linear maps have been obtained recently [13]–[15], [18]. These results have in common the obtaining of an analytical expression for the autocorrelation sequence (ACS) using the n-th iterate of these maps. Consequently, the PSD is obtained using the discrete-time Fourier transform (DTFT) of the ACS. This is not always a trivial task. Here we presented

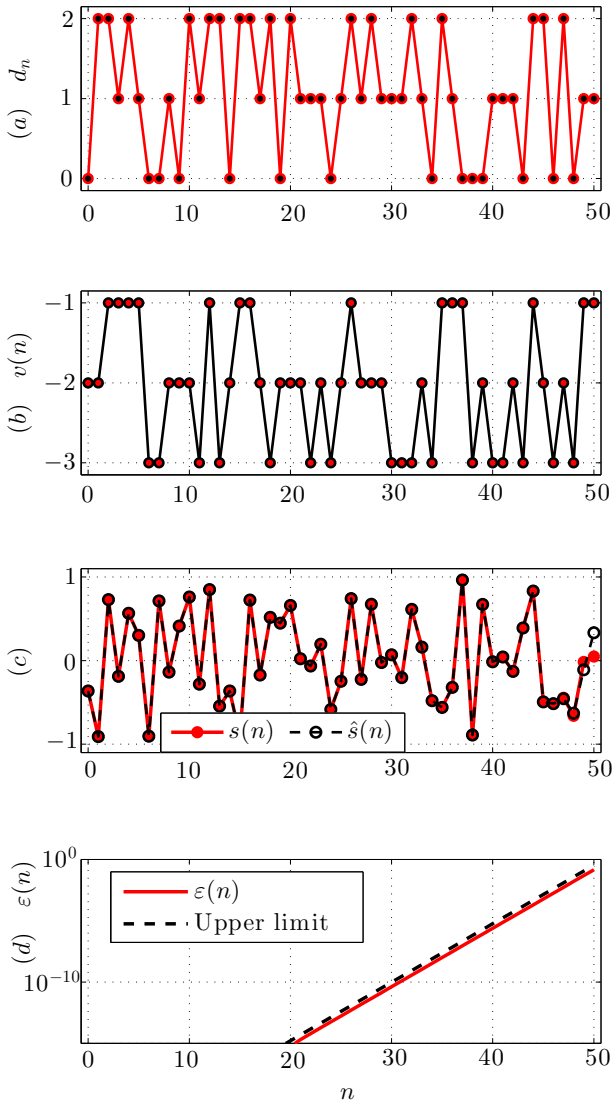

Fig. 2. (a) d_n, (b) $v(n)$, (c) $s(n)$ and $\hat{s}(n)$, (e) $\varepsilon(n)$ for $s(0) = \frac{2}{\pi} - 1$.

another way to calculate the PSD, using the linear systems theory.

The PSD of linear system (13) is given by [19, Ch. 14]

$$S_\ell(\omega) = V(\omega)\,|H(\omega)|^2, \quad (26)$$

where $V(\omega)$ is the PSD of the input sequence $v(n)$, $H(\omega)$ is the frequency response of the recursive filter and $S_\ell(\omega)$ is the PSD of chaotic signals in the output of the linear filter.

The linear system as implemented in Algorithm 1 can be thought as having an independent, identically distributed sequence as entrance with variance σ^2 given by

$$\sigma^2 = \frac{1}{|r|} \sum_{j=0}^{|r|-1} (1-|r|+2j)^2 = \frac{r^2-1}{3}, \quad (27)$$

in which $j = 0, 1, 2, \ldots, |r| - 1$ represents all possible digits in base $|r|$.

So the ACS is

$$R(k) = \sigma^2 \delta(k) \tag{28}$$

where $\delta(\cdot)$ is the Dirac unit impulse function [17].

Using (27) in (28) and taking the DTFT of (28), we obtain

$$V(\omega) = \frac{r^2 - 1}{3}. \tag{29}$$

The linear system (13) can be represented by the transfer function $H(z)$,

$$H(z) = \frac{r^{-1}}{1 - z^{-1} r^{-1}}. \tag{30}$$

Take the module squared from (30) and substituting $z = e^{j\omega}$ we have

$$|H(\omega)|^2 = \frac{1}{r^2 + 1 - 2r\cos(\omega)}. \tag{31}$$

Substituting (31) and (29) in (26) we obtain

$$S_\ell(\omega) = \frac{r^2 - 1}{3\left(1 + r^2 - 2r\cos(\omega)\right)}. \tag{32}$$

This result completely agrees with the obtained using a recursive formula for $f^n(\cdot)$ in [13].

Figure 3 shows the PSD for some values of r. When r is positive, $S_\ell(\omega)$ has maximum at $\omega = 0$ and minimum for $\omega = \pi$, confirming the low-pass properties of the generated signals. Otherwise, when r is negative, $S_\ell(\omega)$ has maximum at $\omega = \pi$ and minimum for $\omega = 0$, resulting in high-pass signals.

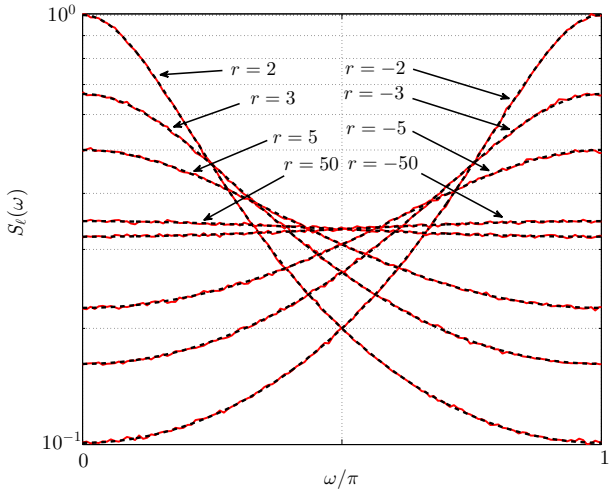

Fig. 3. PSD for some values of r. The analytical results are shown in dashed lines and numerical simulations in continuous lines.

V. Conclusions

In this paper, we extended the linear representation of chaotic signals proposed in [16] including piecewise linear maps with negative slope segments. Besides that, we use the linear systems theory to obtain the PSD of chaotic signals in a straightforward way. Our exact results are in agreement with the numerical simulations and literature [13]. We are currently working in further extending our results to more general piecewise-linear maps.

References

[1] K. T. Alligood, T. D. Sauer, and J. A. Yorke, *Chaos*, ser. Textbooks in Mathematical Sciences. Springer New York, 2000.

[2] R. T. Fontes and M. Eisencraft, "Noise filtering in bandlimited digital chaos-based communication systems," in *22nd European Signal Processing Conference, EUSIPCO 2014, Lisbon, Portugal, September 1-5, 2014*, 2014, pp. 406–410.

[3] R. Candido, M. Eisencraft, and M. T. M. Silva, "Channel equalization for synchronization of Ikeda maps," in *Proc. of* 21st *European Signal Processing Conference (EUSIPCO'2013)*, Marrakesh, Marocco, 2013.

[4] C. E. C. Souza, D. P. B. Chaves, and C. Pimentel, "Digital communication systems based on three-dimensional chaotic attractors," *IEEE Access*, vol. 7, pp. 10 523–10 532, 2019.

[5] H.-P. Ren, M. S. Baptista, and C. Grebogi, "Wireless communication with chaos," *Physical Review Letters*, vol. 110, no. 18, p. 184101, apr 2013.

[6] G. Kaddoum, "Wireless chaos-based communication systems: A comprehensive survey," *IEEE Access*, vol. 4, pp. 2621–2648, 2016.

[7] J.-L. Yao, C. Li, H.-P. Ren, and C. Grebogi, "Chaos-based wireless communication resisting multipath effects," *Physical Review E*, vol. 96, no. 3, sep 2017.

[8] H.-P. Ren, C. Bai, Q. Kong, M. S. Baptista, and C. Grebogi, "A chaotic spread spectrum system for underwater acoustic communication," *Physica A: Statistical Mechanics and its Applications*, vol. 478, pp. 77–92, jul 2017.

[9] H. Xu, Y. Li, J. Zhang, H. Han, B. Zhang, L. Wang, Y. Wang, and A. Wang, "Ultra-wideband chaos life-detection radar with sinusoidal wave modulation," *International Journal of Bifurcation and Chaos*, vol. 27, no. 13, p. 1730046, dec 2017.

[10] Y. Zhou, L. Bao, and C. P. Chen, "A new 1d chaotic system for image encryption," *Signal Processing*, vol. 97, pp. 172–182, apr 2014.

[11] N. A. Loan, N. N. Hurrah, S. A. Parah, J. W. Lee, J. A. Sheikh, and G. M. Bhat, "Secure and robust digital image watermarking using coefficient differencing and chaotic encryption," *IEEE Access*, vol. 6, pp. 19 876–19 897, 2018.

[12] H.-P. Ren, C. Bai, J. Liu, M. S. Baptista, and C. Grebogi, "Experimental validation of wireless communication with chaos," *Chaos: An Interdisciplinary Journal of Nonlinear Science*, vol. 26, no. 8, p. 083117, aug 2016.

[13] R. A. Costa, M. B. Loiola, and M. Eisencraft, "Correlation and spectral properties of chaotic signals generated by a piecewise-linear map with multiple segments," *Signal Processing*, vol. 133, pp. 187–191, apr 2017.

[14] A. Sahnoune and D. Berkani, "On the correlation of chaotic signals generated by multimodal skew tent map," *Signal, Image and Video Processing*, vol. 12, no. 7, pp. 1273–1278, mar 2018.

[15] R. A. da Costa and M. Eisencraft, "Spectral characteristics of a general piecewise linear chaotic signal generator," *Communications in Nonlinear Science and Numerical Simulation*, vol. 72, pp. 441–448, jun 2019.

[16] D. F. Drake and D. B. Williams, "Linear, random representations of chaos," *IEEE Transactions on Signal Processing*, vol. 55, no. 4, pp. 1379–1389, apr 2007.

[17] A. V. Oppenheim and R. W. Schafer, *Discrete-Time Signal Processing*, 3rd ed. Upper Saddle River, NJ, USA: Addison Wesley Pub CO Inc, 2009.

[18] R. A. Costa, M. B. Loiola, and M. Eisencraft, "Spectral properties of chaotic signals generated by the Bernoulli map," *Journal of Engineering Science and Technology Review*, vol. 8, no. 2, pp. 12–16, 2015.

[19] J. G. Proakis and D. K. Manolakis, *Digital Signal Processing (4th Edition)*. Pearson, 2006.